

Time-to-reach Bounds for Verification of Dynamical Systems Using the Koopman Spectrum

Jianqiang Ding and Shankar A. Deka, *Member, IEEE*

Abstract—In this work, we present a novel Koopman spectrum-based reachability verification method for nonlinear systems. Contrary to conventional methods that focus on characterizing all potential states of a dynamical system over a presupposed time span, our approach seeks to verify the reachability by assessing the non-emptiness of estimated time-to-reach intervals without engaging in the explicit computation of reachable set. Based on the spectral analysis of the Koopman operator, we reformulate the problem of verifying existence of reachable trajectories into the problem of determining feasible time-to-reach bounds required for system reachability. By solving linear programming (LP) problems, our algorithm can effectively estimate all potential time intervals during which a dynamical system can enter (and exit) target sets from given initial sets over an unbounded time horizon. Finally, we demonstrate our method in challenging settings, such as verifying the reachability between non-convex or even disconnected sets, as well as backward reachability and multiple entries into target sets. Additionally, we validate its applicability in addressing real-world challenges and scalability to high-dimensional systems through case studies in verifying the reachability of the cart-pole and multi-agent consensus systems.

Index Terms—Koopman operator, reachability analysis, verification, nonlinear dynamical systems.

I. INTRODUCTION

As modern society increasingly relies on complex systems in safety-critical areas such as robotics, autonomous driving, and power grids, providing rigorous guarantees to ensure their reliable operation has become crucial. Formal guarantees typically involve verifying safety, which determines whether all trajectories from the initial set avoid entering the unsafe set, and its dual problem, reachability verification, which checks if at least one trajectory starting from the initial set will reach the target set in finite time [1]. Fundamentally, both types of problems examine whether a valid time horizon exists that allows the system to reach the target set from the initial set.

Verification of reachability for dynamical system has been extensively studied within the control community in recent decades, and numerous methods have been developed for these verification problems where the time horizon is considered a fixed parameter of the problem, alongside the initial set and the target set.

For instance, [2]–[5] take an abstraction-based approach wherein reachability analysis is performed on an abstract representation of the original system. In a different vein, Hamilton-Jacobi (HJ) approaches [6] [7] frame the problem as a two-player zero-sum game between the controller and an adversary, leading to backward reachable set in the form of zero-sublevel set of the solution of a Hamilton-Jacobi partial differential equation, which can be numerically solved with level-set methods [8]. However, the computational complexity of these approaches is exponential in the state dimensions, rendering them intractable for relatively large dimension systems. Therefore, learning-based techniques [9], [10] have recently been applied to boost the scalability and performance of such methods. Other approaches aim to prove that unsafe states are unreachable by finding invariant sets that include the initial set and exclude the unsafe set, which can be synthesized via optimization techniques involving algebraic geometry [11]–[13]. A popular category of methods in this direction achieve verification by constructing barrier functions, which provide Lyapunov-like guarantees regarding system behavior. The existence of a barrier function is sufficient to conclude the satisfiability of safety or reachability specifications [1], [14]–[16]. In addition, set-propagation techniques [17] are also worthy of attention. Starting from initial states, these techniques iteratively compute sets representing all possible behaviors of the system in accordance with its dynamics. A variety of tools [18]–[20] have been developed for reachable set computation in a broad range of dynamical systems, including continuous nonlinear system, hybrid system, and even neural networks. Yet other methodologies based on satisfiability modulo theory (SMT) [21], seek to verify reachability by searching for counterexamples. These approaches has consequently spurred the development of several tools [22], [23] for verification. Technically, as discussed in [24], reachability verification typically relies on computation of finite-time reachable set from an initial set, which is then intersected with the target set. Indeed, exploiting system properties such as monotonicity [25], symmetries [26], [27], and decomposition based on system structures [28], can scale up reachability analysis techniques. However, this explicit computation of reachable sets, which is often expensive and/or conservative, may not be required in principle since the main goal of verification is to obtain a “yes” or “no” answer, and not to obtain actual reachable sets.

In fact, the aforementioned approaches hinge heavily on

Department of Electrical Engineering, Aalto University, Finland.
Email: {jianqiang.ding, shankar.deka}@aalto.fi.

Method	Applicability		Framework		Time Horizon		Set Type for Reachability			Remark
	Model-based	Data-driven	Finite	Infinite	Convex	Non-Convex	Disjoint			
Abstraction-based Techniques [3], [29], [30]	Yes	No	Yes	Limited	Yes	Limited	No	Primarily designed for hybrid systems; Typically discretize the state-space, limiting the number of state variables		
Hamilton-Jacobi PDEs [6], [7]	Yes	Limited	Yes	No	Yes	Yes	Yes	Solved by expensive level set numerical methods; Low scalability for high-dimensional systems		
Deductive Approaches [11], [13], [15], [16]	Yes	Yes	No	Yes	Yes	Yes	Yes	Generally based on proving that unsafe sets are unreachable by constructing invariant sets.		
Set-Propagation Techniques [17]	Yes	Yes	Yes	No	Yes	Limited	No	Mostly restricted to finite time horizon problems; Over-approximation of sets often lead to the wrapping effects		
Counterexamples Searching [22], [23]	Yes	No	Yes	Yes	-	-	-	High computational complexity		
Ours	Yes	Yes	Yes	Yes	Yes	Yes	Yes	Necessary condition; Over-approximation of reach-time bounds		

TABLE I: Comparison of various reachability analysis methodologies in literature.

Note: Reachability analysis algorithms typically blend elements from multiple approaches. Despite varying emphases, algorithms often require ‘set-propagation techniques’ to analyze the reachability based on the characterization of reachable sets. Consequently, the attribute ‘Set Type for Reachability’ reflects the level of support for various types of sets in set propagation.

precise system modeling, which is often difficult to achieve in practice. This gap restricts their application and performance in real-world scenarios. Thus, data-driven approaches are rapidly becoming an important research focus in the control community. Recent research [31], [32] emphasizes characterizing reachable sets in a probabilistic sense to account for noise in data. Other studies can be viewed as extensions of model-based set-propagation approaches. For instance, [33], [34] compute reachable sets using zonotopes based on Willems et al.’s lemma [35] without requiring a priori system model. While such methods do relax the dependency of reachability analysis algorithms on models to a certain extent, their direct use of measurement data and the computation based on set representations restrict their scalability to high-dimensional and complex systems. To tackle these challenges, we propose a novel reachability verification approach based on Koopman spectrum, which eliminates the necessity for explicitly computing reachable sets. The method’s independence from the precise model positions it as a promising foundation for developing efficient and highly scalable reachability verification methodologies for unknown systems when combined with data-driven Koopman operator approximation techniques. Thus, the main contributions of this work are summarized as follows:

- We introduce a novel Koopman spectrum-based necessary condition for reachability verification. This condition reframes the reachability problem as checking whether the time-to-reach bounds are non-empty, thus avoiding explicit computation of reachable sets and mitigates the dependency on precise modeling of the dynamic.
- Building upon this necessary condition, we further relax the estimates of the time-to-reach bounds through parameterization via principal eigenpairs. This relaxation allows the problem can be efficiently solved as linear programming (LP) problems in decision variables that scale linearly with the state-dimensions.
- Finally, we demonstrate the practicality of our approach through several challenging case studies that involve non-convex sets, periodic orbits, and high-dimensional systems.

II. RELATED WORK

Given that linear dynamical systems permit closed-form solutions along with a wide array of techniques for their analysis, prediction, and control, the extension of these methodologies to nonlinear systems through the construction of linear approximations has been a prevailing research focus within the control community.

Unlike local linear approximation techniques such as Taylor series expansion, by representing a nonlinear dynamical systems in terms of an infinite-dimensional operator acting on a Hilbert space of measurement functions of the system state, Koopman operator theory [36] has garnered significant attention in control research due to its ability to achieve global linearization of nonlinear systems. While the Koopman operator is theoretically defined as an infinite-dimensional linear operator, it can be approximated in a finite-dimensional form using techniques like Dynamic Mode Decomposition (DMD) and its various extensions [37] and Krylov-subspace methods [38].

Additionally, considering the critical role of Koopman spectral theory in facilitating the analysis and control of dynamical system, innovative methods such as the path-integral method [39] and Laplace average method [40] [41] have been developed recently to numerically evaluate the principal eigenfunctions over specific domains, and its combination with neural networks [42] has further enhanced flexibility in approximating eigenfunctions, thus providing a more practical framework for the study of dynamical systems.

Naturally, such a Koopman-based perspective of dynamical systems has led to the development of various methodologies for Koopman theory-based reachability analysis. One of the first algorithms in this direction was proposed in [43], where the authors verify the reachability of black-box nonlinear systems with Koopman linearization and zonotope over-approximations of nonlinear initial sets. Subsequently, [44] advance this idea by employing random Fourier features to improve the accuracy of linearization, and combining Taylor models with polynomial zonotope refinement to handle the nonlinear transformation of the initial states. The reachability of the Koopman bilinear form of control-affine nonlinear systems is discussed in [45]. In contrast, other methods seek to utilize the Koopman spectrum to analyze the reachability of the

system. The authors in [46] use the principal eigenfunctions of the Koopman operator for the characterization of both forward and backward reachable sets, and provide formal guarantees for the set approximation under the Hausdorff metric.

III. PRELIMINARIES

Notations: We use \mathbb{R} and \mathbb{C} to denote the set of real and complex numbers, respectively. \mathbb{R}^n denotes the n -dimensional real space. The space of all k -times continuously differentiable functions on domain X is denoted by $C^k(X)$. The notation $\text{spec}(M)$ denotes the spectrum of a matrix $M \in \mathbb{C}^{n \times n}$. $\text{Re}(\cdot)$ and $\text{Im}(\cdot)$ denote the real and imaginary parts of an argument, respectively. $|\cdot|$ is used to denote absolute value of a real or complex number and likewise $\angle \cdot$ denotes the phase angle of a complex scalar.

In this paper, we consider continuous-time dynamical systems of the form

$$\frac{d}{dt}x(t) = f(x(t)) \quad (1)$$

where $f : X \rightarrow \mathbb{R}^n$ is a continuously differentiable map and $x(t) \in \mathbb{R}^n$ denotes the state in the compact set $X \in \mathbb{R}^n$ at time $t \geq 0$. The flow map $s_t : X \rightarrow X$ of system (1) is given by $s_t(x) = x + \int_0^t f(x(\tau))d\tau$, for all $t \geq 0$ and $x \in X$.

Assumption 1. *Unless otherwise noted, we assume that x_e is a hyperbolic equilibrium point of the system (1), i.e., $A = \frac{\partial f}{\partial x}(x_e)$ has no eigenvalues on the imaginary axis in the complex plane, to ensure that principal eigenfunctions and the corresponding eigenvalues are well-defined near equilibrium points and can be computed numerically by analyzing the linearization of the system. Furthermore, we assume that the equilibrium point and points on the limit cycles is not contained within the initial set and the target set.*

Definition 1. (Koopman Operator) Let \mathcal{F} be a Banach space of scalar-valued functions $\phi(x) : X \rightarrow \mathbb{C}$. Then, the Koopman operator $\mathbb{U}_t : \mathcal{F} \rightarrow \mathcal{F}$ corresponding to the dynamics (1) is defined as

$$[\mathbb{U}_t\phi](x) = \phi(s_t(x)) \quad (2)$$

where $\phi(x) \in \mathcal{F}$ commonly refers to as an observable function. We assume $\mathcal{F} \subseteq C^1(X)$ in this paper.

Definition 2. (Koopman Eigenvalues and Eigenfunctions) An observable function $\phi(x) \in \mathcal{F}$ is said to be an eigenfunction of the Koopman operator corresponds to the eigenvalue λ if

$$[\mathbb{U}_t\phi](X) = e^{\lambda t}\phi(x), \quad t \geq 0. \quad (3)$$

With the Koopman generator, \mathcal{K}_f , equation (3) can be written as

$$\mathcal{K}_f\phi = \frac{\partial\phi}{\partial x}f(x) = \lambda\phi(x) \quad (4)$$

In addition to being defined for all $t \in [0, \infty)$ and $x \in X$, the Koopman spectrum can be generalized to finite time and the subset of state space as open and subdomain eigenfunctions.

Definition 3. (Open and Subdomain Eigenfunctions [47]) Let $\phi : B \rightarrow \mathbb{C}$, where $B \subset X$ is not an invariant set. Let $x \in B$, and $\tau \in (\tau^-(x), \tau^+(x)) = I_x$, a connected open interval such that $s_\tau(x) \in B$ for all $\tau \in I_x$, If

$$[\mathbb{U}_\tau\phi](x) = \phi(s_\tau(x)) = e^{\lambda\tau}\phi(x), \quad \forall \tau \in I_x, \quad (5)$$

then $\phi(x)$ is called an open eigenfunction of the Koopman operator with eigenvalue λ . If B is the proper invariant subset of X (i.e., $I_x = \mathbb{R}$ for all $x \in B$), then $\phi(x)$ is called subdomain eigenfunction.

Remark 1. If $B = X$, then $\phi(x)$ will be an ordinary eigenfunction associated with eigenvalue λ as defined in (3). When B is open, the open eigenfunctions as defined above can be extended from B to a larger set which is the backward reachable from the closure of B , based on the construction procedure outlined in [47].

Let \mathcal{D} be the domain of attraction of the equilibrium point. We focus on the reachability verification problem of system (1) within domain \mathcal{D} that satisfies Assumption 1. The existence of a hyperbolic equilibrium enables the analysis of nonlinear behavior via its linearization around the equilibrium point by applying Hartman-Grobman theorem [48], [49]. In the following, we will refer to the eigenfunctions of the Koopman operator associated with the eigenvalues of the linearized system as *principal eigenfunctions*. Furthermore, we define the set of principal eigenpairs as the minimal generator G of the set given by

$$E = \left\{ \left(\sum_{i=1}^m n_i \lambda_i, \prod_{i=1}^m \phi_i^{n_i} \right) \mid (\lambda_i, \phi_i) \in G, n_i \in \mathbb{N} \right\}.$$

where E is the semigroup of eigenpairs (λ, ϕ) .

The concept of principal eigenfunctions was introduced in [50], and uniqueness and existence of these principal eigenfunctions have been studied rigorously in [51]. Due to its principal algebraic structure, the cardinality of set E is countably infinite. As pointed out in [52], this set doesn't contain all the possible Koopman eigenfunctions, and the authors consequently introduced the concept of 'primary eigenfunctions,' to allow the exponents n_i in the definition of set E above to be real valued. We shall follow this extension by [52] for parameterizing the Koopman spectrum in our paper.

IV. TIME-TO-REACH BOUNDS

Consider a set of initial conditions $X_0 \subset X$ and a target final set $X_F \subset X$ such that $x_e \notin X_0 \cup X_F$. Additionally, given any function $g : X \rightarrow \mathbb{R}$ and a set $V, W \subset X$, let us define the following notations for convenience:

$$\bar{g}(V) \doteq \sup_{x \in V} g(x), \quad \underline{g}(V) \doteq \inf_{x \in V} g(x) \quad (6)$$

$$\mathcal{L}^g(W, V) \doteq \log \left(\frac{\bar{g}(V)}{\underline{g}(W)} \right) \quad (7)$$

Let us first consider a real-valued Koopman eigenfunction $\psi \in \mathcal{F}$, corresponding to eigenvalue $\lambda \in \mathbb{R}$. Thus, we can now state the following theorem on time-to-reach bounds.

Theorem 1. A necessary condition for the target set X_F to be reachable from an initial set X_0 is that all the intervals

$$I(\lambda, \psi) \doteq \begin{cases} \left[-\frac{1}{|\lambda|} \mathcal{L}^\psi(X_F, X_0), \frac{1}{|\lambda|} \mathcal{L}^\psi(X_0, X_F) \right] & \text{if } \lambda > 0, \\ \left[-\frac{1}{|\lambda|} \mathcal{L}^\psi(X_0, X_F), \frac{1}{|\lambda|} \mathcal{L}^\psi(X_F, X_0) \right] & \text{if } \lambda < 0. \end{cases}$$

generated from Koopman eigenpairs have a non-empty intersection. In other words,

$$\begin{aligned} s_t(X_0) \cap X_F &\neq \emptyset \text{ for some } t > 0 \\ \implies \bigcap_{(\lambda, \psi) \in E} I(\lambda, \psi) &\neq \emptyset \end{aligned} \quad (8)$$

Proof. Let x_0 be some point in X_0 such that $s_T(x_0) \in X_F$ for some $T > 0$. By definition, we have $\psi(s_T(x_0)) = e^{\lambda T} \psi(x_0)$. For unstable eigenfunctions ($\lambda > 0$), this implies

$$\begin{aligned} e^{\lambda T} \underline{\psi}(X_0) &\leq \overline{\psi}(X_F) \text{ and} \\ e^{\lambda T} \overline{\psi}(X_0) &\geq \underline{\psi}(X_F), \end{aligned}$$

where the underbar and the overbar notations are as defined in (6). Following this, we obtain the bounds on T as:

$$\begin{aligned} -\frac{1}{|\lambda|} \mathcal{L}^\psi(X_F, X_0) &\leq T \leq \frac{1}{|\lambda|} \mathcal{L}^\psi(X_0, X_F) \text{ if } \lambda > 0, \\ -\frac{1}{|\lambda|} \mathcal{L}^\psi(X_F, X_0) &\leq -T \leq \frac{1}{|\lambda|} \mathcal{L}^\psi(X_0, X_F) \text{ if } \lambda < 0. \end{aligned} \quad (9)$$

For notational brevity, we shall denote the lower bound for T obtained in equation (9) as $\underline{T}(\lambda, \psi)$, whereas the upper bound is denoted by $\overline{T}(\lambda, \psi)$. We note that both $\underline{T}(\lambda, \psi)$ and $\overline{T}(\lambda, \psi)$ are well-defined (due to extreme value theorem) and furthermore, are strictly positive. This is because we consider eigenfunction ψ to be continuous on the compact sets X_0, X_F which do not contain the equilibrium point, and therefore ψ is finite and strictly bounded away from zero on the sets X_0, X_F . This holds true even if X_F is not reachable from X_0 .

Finally, since the time to reach X_F from X_0 must satisfy the bounds (9) for every (real-valued) Koopman eigenpair $(\lambda, \psi) \in E$, we have $T \in \bigcap_{(\lambda, \psi) \in E} I(\lambda, \psi)$. \square

The right-hand side of equation (8) means that

$$\begin{aligned} \max \left\{ \sup_{(\lambda, \psi) \in E_u} -\frac{1}{\lambda} \mathcal{L}^\psi(X_F, X_0), \sup_{(\lambda, \psi) \in E_s} \frac{1}{\lambda} \mathcal{L}^\psi(X_0, X_F) \right\} &\leq \\ \min \left\{ \inf_{(\lambda, \psi) \in E_u} \frac{1}{\lambda} \mathcal{L}^\psi(X_0, X_F), \inf_{(\lambda, \psi) \in E_s} -\frac{1}{\lambda} \mathcal{L}^\psi(X_F, X_0) \right\}, \end{aligned}$$

where E_u and E_s denote the subsets of E with unstable and stable real eigenpairs, respectively.

A. Time-bounds parameterized through principal eigenfunctions

Verifying reachability using theorem 1 involves taking intersections of (possibly) an infinite number of intervals. Towards making this procedure conducive to practical implementation, we shall first parameterize $I(\lambda, \psi)$ by parameterizing the eigenpair (λ, ψ) .

Theorem 2. Consider a real (and non-trivial) eigenpair $(\lambda, \psi) \in E$, parameterized by principal eigenpairs as $\psi = \prod_{i=1}^n \psi_i^{\alpha_i}$ and $\lambda = \sum_{i=1}^n \alpha_i \lambda_i$, where $\alpha_i \geq 0$, we have

(a) For $\lambda > 0$:

$$I(\lambda, \psi) \subseteq \left[\frac{\sum_{i=1}^n \alpha_i \mathcal{L}^{\psi_i}(X_F, X_0)}{-\sum_{i=1}^n \alpha_i \lambda_i}, \frac{\sum_{i=1}^n \alpha_i \mathcal{L}^{\psi_i}(X_0, X_F)}{\sum_{i=1}^n \alpha_i \lambda_i} \right]$$

(b) For $\lambda < 0$:

$$I(\lambda, \psi) \subseteq \left[\frac{\sum_{i=1}^n \alpha_i \mathcal{L}^{\psi_i}(X_0, X_F)}{\sum_{i=1}^n \alpha_i \lambda_i}, \frac{\sum_{i=1}^n \alpha_i \mathcal{L}^{\psi_i}(X_F, X_0)}{-\sum_{i=1}^n \alpha_i \lambda_i} \right]$$

Proof. Since logarithm is a monotonically increasing function, we can swap the order of log and sup, such that for any set $S \subseteq X$, we have

$$\begin{aligned} \log \sup_{x \in S} \psi(x) &= \sup_{x \in S} \log \psi(x) = \sup_{x \in S} \sum_{i=1}^n \alpha_i \log \psi_i(x) \\ &\leq \sum_{i=1}^n \alpha_i \sup_{x \in S} \log \psi_i(x) = \sum_{i=1}^n \alpha_i \log \sup_{x \in S} \psi_i(x). \end{aligned}$$

The inequality above follows from the triangular inequality on the sup-norm. In other words,

$$\log \overline{\psi}(S) \leq \sum_{i=1}^n \alpha_i \log \overline{\psi}_i(S). \quad (10)$$

Similarly, we can show that

$$\log \underline{\psi}(S) \geq \sum_{i=1}^n \alpha_i \log \underline{\psi}_i(S). \quad (11)$$

Now using equations (10) and (11) in equation (9), we get the following for $\lambda > 0$:

$$\begin{aligned} -\frac{1}{|\lambda|} \mathcal{L}^\psi(X_F, X_0) &= \frac{1}{\lambda} \log \left(\frac{\underline{\psi}(X_F)}{\overline{\psi}(X_0)} \right) \\ &= \frac{1}{\lambda} (\log(\underline{\psi}(X_F)) - \log(\overline{\psi}(X_0))) \\ &\geq \frac{1}{\lambda} \left(\sum_{i=1}^n \alpha_i \log \underline{\psi}_i(X_F) - \sum_{i=1}^n \alpha_i \log \overline{\psi}_i(X_0) \right) \\ &= \frac{\sum_{i=1}^n \alpha_i \log \left(\frac{\underline{\psi}_i(X_F)}{\overline{\psi}_i(X_0)} \right)}{\sum_{i=1}^n \alpha_i \lambda_i} = \frac{\sum_{i=1}^n \alpha_i \mathcal{L}^{\psi_i}(X_F, X_0)}{-\sum_{i=1}^n \alpha_i \lambda_i}, \end{aligned} \quad (12)$$

$$\begin{aligned} \frac{1}{|\lambda|} \mathcal{L}^\psi(X_0, X_F) &= \frac{1}{\lambda} \log \left(\frac{\overline{\psi}(X_F)}{\underline{\psi}(X_0)} \right) \\ &\leq \frac{1}{\lambda} \left(\sum_{i=1}^n \alpha_i \log \overline{\psi}_i(X_F) - \sum_{i=1}^n \alpha_i \log \underline{\psi}_i(X_0) \right) \\ &= \frac{\sum_{i=1}^n \alpha_i \log \left(\frac{\overline{\psi}_i(X_F)}{\underline{\psi}_i(X_0)} \right)}{\sum_{i=1}^n \alpha_i \lambda_i} = \frac{\sum_{i=1}^n \alpha_i \mathcal{L}^{\psi_i}(X_0, X_F)}{\sum_{i=1}^n \alpha_i \lambda_i}. \end{aligned} \quad (13)$$

In the same way, for the case of $\lambda < 0$, we have

$$-\frac{1}{|\lambda|} \mathcal{L}^\psi(X_0, X_F) \geq \frac{\sum_{i=1}^n \alpha_i \log\left(\frac{\psi_i(X_0)}{\psi_i(X_F)}\right)}{-\sum_{i=1}^n \alpha_i \lambda_i} \quad (14)$$

$$\frac{1}{|\lambda|} \mathcal{L}^\psi(X_F, X_0) \leq \frac{\sum_{i=1}^n \alpha_i \log\left(\frac{\psi_i(X_0)}{\psi_i(X_F)}\right)}{-\sum_{i=1}^n \alpha_i \lambda_i}. \quad (15)$$

This completes our proof. \square

Corollary 1. Let $\hat{I}(\lambda, \psi)$ be the over-approximation of $I(\lambda, \psi)$ obtained in theorem 2. If $\bigcap_{(\lambda, \psi) \in E} \hat{I}(\lambda, \psi) = \emptyset$, then X_F is unreachable from X_0 .

Proof. Assume there exists a trajectory starts from X_0 and reach the target set X_F for some $T > 0$. By theorem 1, we then have $\bigcap_{(\lambda, \psi) \in E} I(\lambda, \psi) \neq \emptyset$. But since $I(\lambda, \psi) \subseteq \hat{I}(\lambda, \psi)$ for all $(\lambda, \psi) \in E$, it follows that

$$\bigcap_{(\lambda, \psi) \in E} I(\lambda, \psi) \subseteq \bigcap_{(\lambda, \psi) \in E} \hat{I}(\lambda, \psi) = \emptyset$$

which leads to a contradiction. Therefore, X_F cannot be reached from X_0 . \square

Note that the over-approximations of $I(\lambda, \psi)$ as presented in theorem 2 are tight, and equality occurs when the principal eigenfunctions ψ_i s can be maximized/minimized over the domains X_0 and X_F independently of one another. The next example illustrates this point numerically.

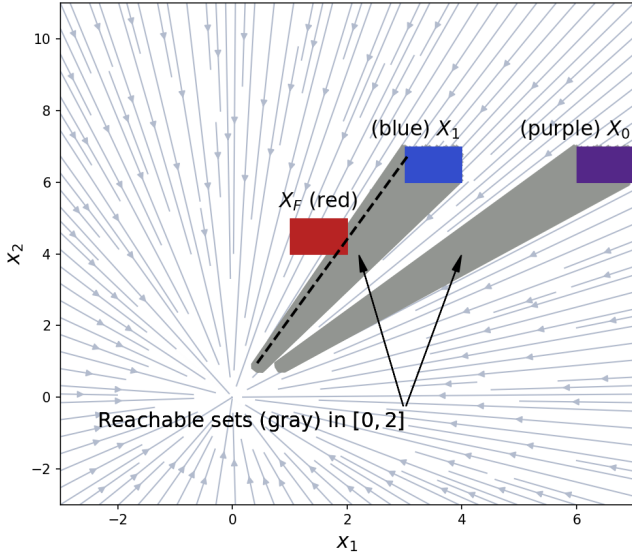


Fig. 1: Reachable sets of the stable linear system from initial sets X_0 and X_1 for duration $T = [0, 2]$ (gray). Simulated trajectory (black dashed line) successfully reaches X_F .

Example 1. (Stable linear system) Consider a linear system

$$\begin{bmatrix} \dot{x}_1 \\ \dot{x}_2 \end{bmatrix} = \begin{bmatrix} -1 & 0 \\ 0 & -1 \end{bmatrix} \begin{bmatrix} x_1 \\ x_2 \end{bmatrix}.$$

Let $X_F = [1, 2] \times [4, 5]$ be the target set. We first consider a set of initial conditions $X_0 = [6, 7] \times [6, 7]$. The principal

eigenfunctions of this system are $\psi_1(x) = x_1$ and $\psi_2(x) = x_2$, with both eigenvalues $\lambda_1, \lambda_2 = -1$. We have $I(\lambda_1, \psi_1) = I(-1, x_1) = [\log(3), \log(7)]$ and $I(\lambda_2, \psi_2) = I(-1, x_2) = [\log(\frac{6}{5}), \log(\frac{7}{4})]$. Clearly, $I(-1, x_1) \cap I(-1, x_2) = \emptyset$. By corollary 1, this implies that the target set X_F cannot be reached from the initial set X_0 since the necessary condition (8) does not hold. Indeed, this can be verified to be true, based on the explicit solution of the linear system. Now, let us now consider another initial set $X_1 = [3, 4] \times [6, 7]$ and compute $I(\lambda, \psi)$ for every eigenpair in E . Any eigenfunction of our system can be expressed in terms of the principal eigenfunction as $\psi = x_1^{\alpha_1} x_2^{\alpha_2}$ corresponding to the eigenvalue $-(\alpha_1 + \alpha_2)$, where $\alpha_1, \alpha_2 \in \mathbb{N}$. Note that we exclude the trivial eigenfunction, wherein α_1 and α_2 are both zero. Thus, we have

$$\begin{aligned} \underline{T}(\lambda, \psi) &= \frac{1}{\alpha_1 + \alpha_2} \left[\log\left(\frac{3^{\alpha_1} 6^{\alpha_2}}{2^{\alpha_1} 5^{\alpha_2}}\right) \right], \\ \overline{T}(\lambda, \psi) &= \frac{1}{\alpha_1 + \alpha_2} \left[\log\left(\frac{4^{\alpha_1} 7^{\alpha_2}}{1^{\alpha_1} 4^{\alpha_2}}\right) \right] \end{aligned}$$

Note that $\underline{T}(\lambda, \psi)$ can be written as $a \log(\frac{3}{2}) + (1-a) \log(\frac{6}{5})$ and similarly, $\overline{T}(\lambda, \psi)$ can be written $a \log(\frac{4}{1}) + (1-a) \log(\frac{7}{4})$, where $a \doteq \frac{\alpha_1}{\alpha_1 + \alpha_2}$. Clearly, for any value of $a \in [0, 1]$, we have $\underline{T}(\lambda, \psi) < \log(\frac{8}{5}) < \overline{T}(\lambda, \psi)$. Thus,

$$\log\left(\frac{8}{5}\right) \in \bigcap_{(\lambda, \psi) \in E} I(\lambda, \psi),$$

which is consistent with the fact that X_F is reachable from X_1 , as indicated by the necessary condition (8).

B. Time-bounds using the eigenfunction phases

In case of complex eigenfunctions, one can utilize information encoded in the phase (or argument) of the eigenfunctions and the imaginary part of the corresponding eigenfunction in addition to its modulus, for further refining the time intervals $I(\lambda, \psi)$. For brevity of presentation, let us introduce the notation $\mathcal{A}^g(W, V) \doteq \overline{\angle g(V)} - \underline{\angle g(W)}$ given any function $g : X \rightarrow \mathbb{C}$ and sets $V, W \subset X$. Thus, we present the following result for reach bounds in terms of the Koopman eigenfunction phase.

Theorem 3. If a set X_F is reachable from an initial set X_0 , then the time-to-reach, T , would necessarily satisfy

$$\text{Im}(\lambda)T \in \left[-\mathcal{A}^\psi(X_F, X_0), \mathcal{A}^\psi(X_0, X_F) \right] + 2m\pi$$

for some $m \in \mathbb{Z}$.

Proof. For any $x \in X_0$ and $t \geq 0$, we have

$$\begin{aligned} \psi(s_t(x)) &= e^{\lambda t} \psi(x) = |\psi(x)| e^{\text{Re}(\lambda)t} e^{j \text{Im}(\lambda)t + j \angle \psi(x)} \\ \implies \angle \psi(s_t(x)) &= \angle \psi(x) + \text{Im}(\lambda)t - 2m\pi \end{aligned}$$

for some $m \in \mathbb{Z}$, where $\angle \psi$ is a function denoting the phase of ψ . Now, if $\exists T > 0$ such that $s_T(x) \in X_F$, then we have

$$\begin{aligned} \overline{\angle \psi}(X_F) &\geq \angle \psi(s_T(x)) = \angle \psi(x) + \text{Im}(\lambda)T - 2m\pi \\ &\geq \underline{\angle \psi}(X_0) + \text{Im}(\lambda)T - 2m\pi \\ \implies \text{Im}(\lambda)T &\leq \overline{\angle \psi}(X_F) - \underline{\angle \psi}(X_0) + 2m\pi. \end{aligned}$$

Similarly,

$$\begin{aligned} \underline{\angle\psi}(X_F) &\leq \angle\psi(s_T(x)) = \angle\psi(x) + \text{Im}(\lambda)T - 2m\pi \\ &\leq \overline{\angle\psi}(X_0) + \text{Im}(\lambda)T - 2m\pi \\ \implies \text{Im}(\lambda)T &\geq \underline{\angle\psi}(X_F) - \overline{\angle\psi}(X_0) + 2m\pi. \end{aligned}$$

This completes the proof. \square

We shall denote the time-to-reach interval in theorem 3 as $I_{phase}(\lambda, \psi)$. Just like in the case of real eigenpairs, one can parameterize this interval using the principal Koopman spectrum as follows.

Theorem 4. *Given a complex (and non-trivial) eigenpair $(\lambda, \psi) \in E$, parameterized by $\psi = \prod_{i=1}^n \psi_i^{\alpha_i}$ and $\lambda = \sum_{i=1}^n \alpha_i \lambda_i$, where $\alpha_i \geq 0$, we have*

(a) For $\text{Im}(\lambda) > 0$, and some $m \in \mathbb{Z}$,

$$I_{phase}(\lambda, \psi) \in \left[\frac{\sum_{i=1}^n \alpha_i \mathcal{A}^{\psi_i}(X_0, X_F) + 2m\pi}{\sum_{i=1}^n \alpha_i \text{Im}(\lambda_i)}, \frac{\sum_{i=1}^n -\alpha_i \mathcal{A}^{\psi_i}(X_F, X_0) + 2m\pi}{\sum_{i=1}^n \alpha_i \text{Im}(\lambda_i)} \right]$$

(b) For $\text{Im}(\lambda) < 0$, and some $m \in \mathbb{Z}$,

$$I_{phase}(\lambda, \psi) \in \left[\frac{\sum_{i=1}^n \alpha_i \mathcal{A}^{\psi_i}(X_F, X_0) + 2m\pi}{-\sum_{i=1}^n \alpha_i \text{Im}(\lambda_i)}, \frac{\sum_{i=1}^n \alpha_i \mathcal{A}^{\psi_i}(X_0, X_F) + 2m\pi}{\sum_{i=1}^n \alpha_i \text{Im}(\lambda_i)} \right]$$

Proof. We begin by noting that $\angle \prod_{i=1}^n \psi_i^{\alpha_i} = \sum_{i=1}^n \alpha_i \angle \psi_i + 2k\pi$ for some $k \in \mathbb{Z}$. For any set $S \subseteq X$, this gives us

$$\begin{aligned} \overline{\angle\psi}(S) &= \sup_{x \in S} \angle\psi(x) = \sup_{x \in S} \sum_{i=1}^n \alpha_i \angle\psi_i(x) + 2k\pi \\ &\stackrel{\text{triangular inequality}}{\leq} \sum_{i=1}^n \sup_{x \in S} \alpha_i \angle\psi_i(x) + 2k\pi \\ &= \sum_{i=1}^n \alpha_i \overline{\angle\psi_i}(S) + 2k\pi, \text{ and similarly} \\ \underline{\angle\psi}(S) &\stackrel{\text{triangular inequality}}{\geq} \sum_{i=1}^n \alpha_i \underline{\angle\psi_i}(S) + 2k\pi. \end{aligned}$$

Therefore,

$$\begin{aligned} \mathcal{A}^{\psi}(X_0, X_F) &\leq \sum_{i=1}^n \alpha_i \overline{\angle\psi_i}(X_F) - \sum_{i=1}^n \alpha_i \underline{\angle\psi_i}(X_0) \text{ and} \\ -\mathcal{A}^{\psi}(X_F, X_0) &\geq \sum_{i=1}^n \alpha_i \underline{\angle\psi_i}(X_F) - \sum_{i=1}^n \alpha_i \overline{\angle\psi_i}(X_0) \end{aligned}$$

The rest of the proof follows simply by using these above inequalities in the expression for I_{phase} obtained from theorem 3 for the two cases ($\text{Im}(\lambda) < 0$ and $\text{Im}(\lambda) > 0$). \square

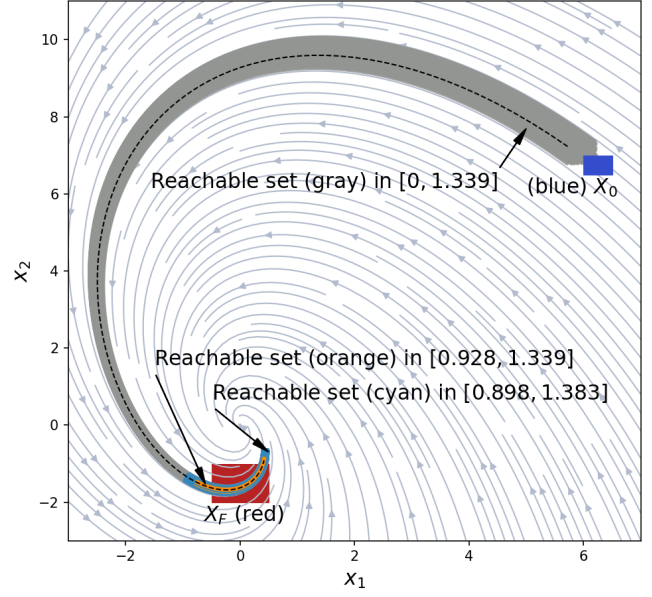


Fig. 2: Reachable sets of the stable linear spiral system from initial set X_0 for duration $T_0 = [0, 1.339]$ (gray), $T_1 = [0.928, 1.339]$ (orange), $T_2 = [0.898, 1.383]$ (cyan), and simulated trajectory (black dashed line).

Example 2. (Stable linear spiral system) Consider a linear system

$$\begin{bmatrix} \dot{x}_1 \\ \dot{x}_2 \end{bmatrix} = \begin{bmatrix} -3 & -2 \\ 7 & -1 \end{bmatrix} \begin{bmatrix} x_1 \\ x_2 \end{bmatrix}.$$

The system has complex principal eigenvalues $\lambda_1 = -2 + 3.606j$ and $\lambda_2 = \lambda_1^*$. Given the initial set and target set as $X_0 = [6, 6.5] \times [6.5, 7]$ and $X_F = [-0.5, 0.5] \times [-2, -1]$, the values of each principal eigenfunction within X_0 and X_F are numerically computed using the path-integral method [39]. Based on the modulus values, we obtain the estimated reachable time interval $I_{modulus} = [0.898, 1.383]$. By considering the phase values of the principal eigenfunctions and the imaginary parts of the corresponding eigenvalues, we can estimate the periodic distribution of reachable time intervals, denoted as $I_{phase} = [-0.815, -0.403]$ with a period $P = 1.743$. Taking the intersection of $I_{modulus}$ and $I_{phase} + mP \forall m \in \mathbb{Z}$ we obtain a much tighter estimate $I = [0.928, 1.339]$, which is consistent with the simulation result shown in Fig. 2.

Remark 2. Note that, although the motivation of our algorithm stems from estimating reach-time bounds, its upper bound also represents the latest time the system remains within the target sets. In other words, our method estimates both the reach-time and the duration within the target sets.

C. Numerical implementation

As previously mentioned in theorems 2 and 4, we can estimate the upper and lower bounds of the reachable time interval, by exploring all possible $\alpha_i \in [0, +\infty)$, $i = 1, \dots, n$, which parameterize all Koopman eigenfunctions and eigenvalues in terms of the principal Koopman spectrum. For reachable

time bounds derived from the real parts of principal eigenfunctions, the determination of each lower (upper) bound essentially defines a linear-fractional programming (LFP) problem to maximize (minimize) a ratio of affine functions as follows,

$$\begin{aligned} \text{PROBLEM I:} \quad & \max_{z \in \mathbb{R}^n} \frac{c^T z + e}{d^T z + f} \\ & \text{s.t. } Az \leq b \end{aligned}$$

where $c, d \in \mathbb{R}^n$, $b \in \mathbb{R}^m$, $A \in \mathbb{R}^{m \times n}$ and $e, f \in \mathbb{R}$ are constants. By applying the Charnes-Cooper transformation, this LFP problem can be effectively solved as the following linear programming (LP) problem,

$$\begin{aligned} \text{PROBLEM II:} \quad & \max_{y \in \mathbb{R}^n} c^T y + et \\ & \text{s.t. } Ay \leq bt, \\ & d^T y + ft = 1, \\ & t \geq 0, \end{aligned}$$

Lemma 1 (In [53], page 183). *If z^* is an optimal solution of PROBLEM I such that $d^T z^* + f > 0$, and if (y^*, t^*) is an optimal solution of PROBLEM II, then y^*/t^* is an optimal solution of PROBLEM I.*

We can now present our algorithm for computing reach-time bounds. Algorithm 1 utilizes the modulus of the eigenfunctions as follows.

Algorithm 1 Reach-time Bounds Estimation with Modulus

Input: Evaluations of principal eigenfunctions on the initial set $\Psi(X_0) = [\psi_0(X_0), \dots, \psi_n(X_0)]$ and target set $\Psi(X_F) = [\psi_0(X_F), \dots, \psi_n(X_F)]$, corresponding principal eigenvalues $\lambda = [\lambda_0, \dots, \lambda_n]$

Output: Reach-time bounds $I_{modulus}$

```

function LFP( $A, b, c, d, lx, ux$ )
  // linear fractional programming
   $x^* \leftarrow \arg \min_x \frac{c^T x}{d^T x}$ 
  s.t.  $Ax \leq b$ 
   $lx \leq x \leq ux$ 
   $v^* \leftarrow \frac{c^T x^*}{d^T x^*}$ 
  return  $v^*, x^*$ 
end function

```

```

 $\underline{\Psi}(X_0), \overline{\Psi}(X_0) \leftarrow \log |\Psi(X_0)|, \overline{\log} |\Psi(X_0)|$ 
 $\underline{\Psi}(X_F), \overline{\Psi}(X_F) \leftarrow \log |\Psi(X_F)|, \overline{\log} |\Psi(X_F)|$ 
 $\Lambda \leftarrow \text{diag}(\text{Re}(\lambda))$  // Arrange vector into diagonal matrix

```

```

// in the case of positive eigenvalue
 $\underline{I}_{unstable, -} \leftarrow \text{LFP}(-\Lambda, \mathbf{0}, \underline{\Psi}(X_F) - \overline{\Psi}(X_0), \Lambda, \mathbf{0}, 1)$ 
 $\overline{I}_{unstable, -} \leftarrow \text{LFP}(-\Lambda, \mathbf{0}, \overline{\Psi}(X_F) - \underline{\Psi}(X_0), -\Lambda, \mathbf{0}, 1)$ 

```

```

// in the case of negative eigenvalue
 $\underline{I}_{stable, -} \leftarrow \text{LFP}(\Lambda, \mathbf{0}, \overline{\Psi}(X_F) - \underline{\Psi}(X_0), \Lambda, \mathbf{0}, 1)$ 
 $\overline{I}_{stable, -} \leftarrow \text{LFP}(\Lambda, \mathbf{0}, \underline{\Psi}(X_F) - \overline{\Psi}(X_0), -\Lambda, \mathbf{0}, 1)$ 

```

```

 $I_{modulus} \leftarrow [\underline{I}_{unstable}, \overline{I}_{unstable}] \cap [\underline{I}_{stable}, \overline{I}_{stable}]$ 

```

When the eigenfunctions are complex, as indicated in theorem 4, the estimated reach-time bounds based on the phase information can be periodically distributed. Therefore, our goal is to identify the reach-time bound for one cycle and the corresponding period. To achieve a feasible tightest estimate of one reachable time range within a single period (in the case of $\text{Im}(\lambda) > 0$), we solve the following optimization problem,

$$\begin{aligned} \arg \min_{\alpha_i} \quad & \frac{\sum_{i=1}^n \alpha_i c_i}{\sum_{i=1}^n \alpha_i d_i} \\ \text{s.t.} \quad & \sum_{i=1}^n \alpha_i d_i > 0 \\ & \alpha_i > 0 \end{aligned}$$

where $c_i = \overline{\angle \psi_i}(X_F) - \angle \psi_i(X_F) + \overline{\angle \psi_i}(X_0) - \angle \psi_i(X_0)$ and $d_i = \text{Im}(\lambda_i)$. Given the optimal solution $\alpha^* = \{\alpha_0^*, \dots, \alpha_n^*\}$, the period of the reachable time bounds can be determined as $P = \frac{2\pi}{\sum_{i=1}^n \alpha_i^* \text{Im}(\lambda_i)}$. Computations for the case of $\text{Im}(\lambda) < 0$ are done similarly.

Algorithm 2 Reach-time Bounds Estimation with Phases

Input: Evaluations of principal eigenfunctions on the initial set $\Psi(X_0) = [\psi_0(X_0), \dots, \psi_n(X_0)]$ and target set $\Psi(X_F) = [\psi_0(X_F), \dots, \psi_n(X_F)]$, corresponding principal eigenvalues $\lambda = [\lambda_0, \dots, \lambda_n]$

Output: Reach-time bounds I_{phase} , period P

```

function GetBound( $A, B, c, d$ )
   $I \leftarrow [\sum_{i=1}^n c_i A_i / \sum_{i=1}^n c_i d_i, \sum_{i=1}^n c_i B_i / \sum_{i=1}^n c_i d_i]$ 
   $P \leftarrow 2\pi / \sum_{i=1}^n c_i d_i$ 
  return  $I, P$ 
end function

```

```

 $C \leftarrow [c_0, \dots, c_n]$ 
where  $c_i = \overline{\angle \psi_i}(X_F) - \angle \psi_i(X_F) + \overline{\angle \psi_i}(X_0) - \angle \psi_i(X_0)$ 
 $\Gamma \leftarrow \text{diag}(\text{Im}(\lambda))$  // Arrange vector into diagonal matrix

```

```

// in the case of positive eigenvalue
 $\rightarrow, \alpha_{unstable}^* \leftarrow \text{LFP}(-\Gamma, \mathbf{0}, C, \Gamma, \mathbf{0}, 1)$ 
 $A \leftarrow \underline{\angle \psi_i}(X_F) - \overline{\angle \psi_i}(X_0)$ 
 $B \leftarrow \overline{\angle \psi_i}(X_F) - \underline{\angle \psi_i}(X_0)$ 
 $I_{unstable}, P_{unstable} \leftarrow \text{GetBound}(A, B, \alpha_{unstable}^*, \Gamma)$ 

```

```

// in the case of negative eigenvalue
 $\rightarrow, \alpha_{stable}^* \leftarrow \text{LFP}(\Gamma, \mathbf{0}, C, -\Gamma, \mathbf{0}, 1)$ 
 $A \leftarrow \overline{\angle \psi_i}(X_F) - \underline{\angle \psi_i}(X_0)$ 
 $B \leftarrow \underline{\angle \psi_i}(X_F) - \overline{\angle \psi_i}(X_0)$ 
 $I_{stable}, P_{stable} \leftarrow \text{GetBound}(A, B, \alpha_{stable}^*, \Gamma)$ 

```

```

 $P \leftarrow$  if  $P_{unstable}$  is valid, else  $P_{stable}$ 
 $I_{phase} \leftarrow I_{unstable} \cap I_{stable}$ 

```

The final reach-time bounds estimation is all intersections of $I_{modulus}$ from Algorithm 1 with reach-time bound distribution I_{phase} from Algorithm 2 of period P .

V. CASE STUDIES

In this section, we test our proposed method in addressing challenging reachability verification problems, aiming to demonstrate its broad applicability in the field of reachability analysis. Except for the examples 4 and 5 where the principal eigenfunctions are known in closed-form, the values of principal eigenfunctions over given sets in all other examples are numerically determined using the path-integral formula [39]. Note that our method is independent of the specific choice of estimation technique for obtaining the principal eigenfunctions and one could use, for example, EDMD. All programs are run on an Intel Core i5-13400 CPU with 32GB RAM and solved using Mosek. The computational time for each example are listed in the Table II.

Example			Compute time (s)	
Index	Dim	Case	Principal eigenpairs	Reach-time bounds
2	2	Reach-time bounds with modulus	0.293	0.023
		Reach-time bounds with phases		0.008
3	2	Non-convex sets	0.237	0.268
		Disconnected sets	0.133	0.164
4	2	Periodically reachable	—	0.027
5	2	Backward reachable	—	0.027
		Backward unreachable	—	0.025
6	4	Collision estimation	1.647	0.027
		Stabilization verification	2.181	0.032
7	16	Obstacle avoidance verification	58.661	0.028
		Convergence verification	9.223	0.031

TABLE II: Computational times (seconds) for eigenfunction computation using ‘Path-integral’ method and ‘Reach-time Bounds Estimation’.

A. Non-convex and Disconnected sets

Example 3. (Duffing’s oscillator) Consider the nonlinear dynamics

$$\begin{bmatrix} \dot{x}_1 \\ \dot{x}_2 \end{bmatrix} = \begin{bmatrix} x_2 \\ -0.5x_2 - x_1(x_1^2 - 1) \end{bmatrix},$$

with stable equilibrium points at $(\pm 1, 0)$ and a saddle equilibrium point at $(0, 0)$. We consider the reachability verification problems under two different set configurations. First, we consider two non-convex sets given by $X_0 = h_{-0.75, 1.85, 1.2, 0.05}(x) \leq -0.01$ and $X_F = h_{0.65, 0.25, 3, 4, 0.1}(x) \leq -0.9$, as the initial set and target set, respectively, where $h_{x_1^c, x_2^c, a, b, s}(x) = -(1 - \frac{x_1 - x_1^c}{s} + a(\frac{x_2 - x_2^c}{s})^5 + b(\frac{x_1 - x_1^c}{s})^3) \cdot e^{-((\frac{x_1 - x_1^c}{s})^2 + (\frac{x_2 - x_2^c}{s})^2)}$. Our method estimates the potential reach time interval as $I = [5.052, 5.835]$, the simulation result in Fig. 3 validate this estimation.

Next, we consider an initial set $X_0 = [-0.8, -0.7] \times [1.8, 1.9]$ and a target set $X_F = X_F^0 \cup X_F^1 = [1.0, 1.1] \times [1.0, 1.1] \cup [0.6, 0.7] \times [0.2, 0.3]$ which is the union of two disjoint sets. Our method provides the estimate of the reachable

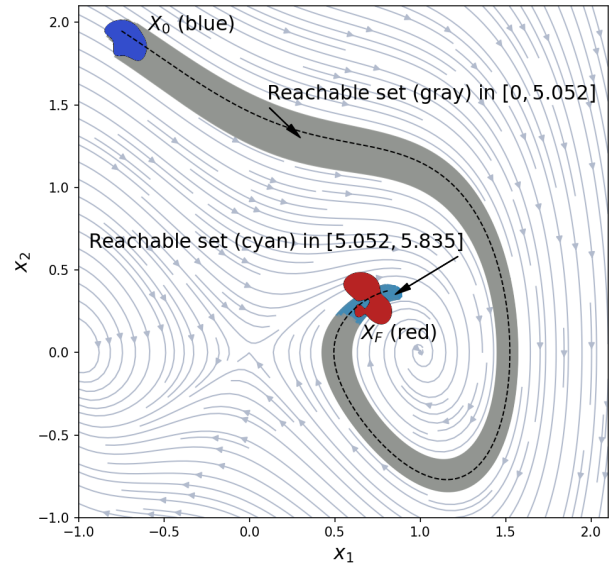


Fig. 3: Reachable sets of the Duffing’s oscillator system from non-convex initial set X_0 for duration $T = [0, 5.052]$ (gray), estimated reach-time bounds $I = [5.052, 5.835]$ (purple) with a simulated reachable trajectory (black dashed line).

time as a union of two disjoint intervals, $I_0 = [0.815, 1.443]$ and $I_1 = [5.009, 5.934]$, indicating the possible existence of trajectories from X_0 that may pass through the disjoint target sets twice. Specifically, the first reach to the target set ranges from 0.815 to 1.443, and the trajectories may re-enter the target set as early as 5.009 and exit no later than 5.934. The simulated trajectories in Fig. 4 corroborate these estimates.

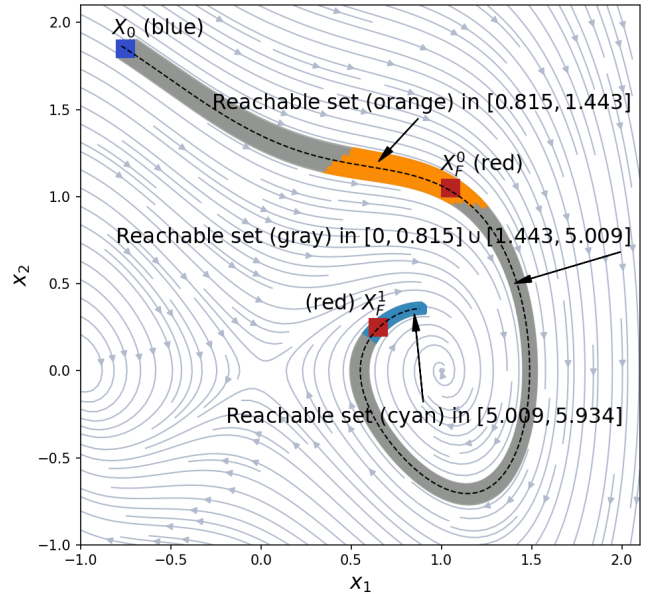


Fig. 4: Reachable set of the Duffing’s oscillator system from initial set X_0 to reach a disjoint target set $X_F = X_F^0 \cup X_F^1$ for duration $T = [0, 0.815] \cup [1.443, 5.009]$ (gray), estimated reach-time bounds $I_0 = [0.815, 1.443]$ (orange), $I_1 = [5.009, 5.934]$ (cyan) with a simulated reachable trajectory (black dashed lines).

B. Periodic and Backward Reachability

A challenge in reachability analysis is determining the long-term behavior of a system, such as verifying its periodic reachability to a target set. Popular approaches like set propagation methods are limited by the inherent wrapping effect and thus cannot verify over extended periods. However, the proposed method leverages the phase of principal eigenfunctions and the imaginary parts of the corresponding eigenvalues to estimate the potential periodic behaviors, allowing us to verify reachability over unbounded time horizons.

Example 4. (System with stable limit cycle) Consider the nonlinear system

$$\begin{bmatrix} \dot{x}_1 \\ \dot{x}_2 \end{bmatrix} = \begin{bmatrix} \frac{-x_1^3 + 4x_1^2 x_2 - x_1 x_2^2 + x_1 + 4x_2^3}{4(x_1^2 + x_2^2)} \\ \frac{-4x_1^3 - x_1^2 x_2 - 4x_1 x_2^2 - x_2^3 + x_2}{4(x_1^2 + x_2^2)} \end{bmatrix}$$

with analytical principal eigenvalues $\lambda_1 = -1 - 1j$ and $\lambda_2 = \lambda_1^*$. The corresponding eigenfunctions are $\psi_1(x) = (1 - x_1^2 - x_2^2)^2 e^{\arctan(x_2/x_1)j}$ and $\psi_2(x) = \psi_1^*(x)$. Since the system has a stable limit cycle $\Gamma = \{x \mid \|x\| = 1\}$, trajectories that originated from the initial set X_0 may periodically pass through the target set X_F multiple times over some time horizon while converging to the limit cycle. To verify reachability under this challenging configuration, we consider the initial set $X_0 = [1.3, 1.4] \times [1.3, 1.4]$ and target set $X_F = [\frac{\sqrt{3}}{2}, \frac{\sqrt{3}}{2} + 0.1] \times [0.5, 0.6]$. Applying our proposed method, we obtain the estimated reach-time bounds as $I_0 = [6.428, 6.625]$ and $I_1 = I_0 + P = [12.711, 12.908]$ where period $P = 6.283$. The visualization in Fig. 5 validates our estimations. We note that, as X_F approaches Γ , $\|\psi_1(X_F)\|$ and $\|\psi_2(X_F)\|$ approach zero and therefore, the reach time interval obtained using eigenfunction modulus (theorem 2) approaches infinity. On the other hand, the reach time estimated using eigenfunction phase (theorem 3) would be $I = I_0 + mP$ with $m \in \mathbb{Z}$, which can intersect $I_{\text{modulus}} = (-\infty, \infty)$ infinite number of times at periodic intervals, giving us periodic reach time estimates when X_F approaches the limit cycle Γ , as one would expect.

Verifying the backward reachability of a system is a common requirement in reachability analysis. It is easy to see that if (ψ_k, λ_k) for $k = 1, \dots, n$ are the principal eigenpairs for system (1), then $(\psi_k, -\lambda_k)$ for $k = 1, \dots, n$ will form the principal eigenpair for the time reversed dynamical system $\dot{x} = -f(x)$. This enables us to apply the proposed method for verifying both forward and backward reachability.

Example 5. (System with known eigenfunction) Consider the dynamics of a two-dimensional system given by

$$\begin{bmatrix} \dot{x}_1 \\ \dot{x}_2 \end{bmatrix} = [\nabla \Psi(x)]^{-1} \begin{bmatrix} -1 & 0 \\ 0 & 2.5 \end{bmatrix} \Psi(x)$$

where the principal eigenfunctions are denoted as $\Psi(x) = [\psi_1(x), \psi_2(x)]^T$ with $\psi_1(x) = x_1^2 + 2x_2 + x_2^3$ and $\psi_2(x) = x_1 + \sin(x_2) + x_1^3$, and the associated eigenvalues are $\lambda_1 = -1$ and $\lambda_2 = 2.5$ at the unstable equilibrium $(0, 0)$. We consider the initial set $X_0 = [0, 0.1] \times [1.1, 1.2]$ and target sets as $X_F^1 = [1.8, 1.9] \times [-0.8, -0.7]$ and $X_F^2 = [1.5, 1.6] \times [0.1, 0.2]$,

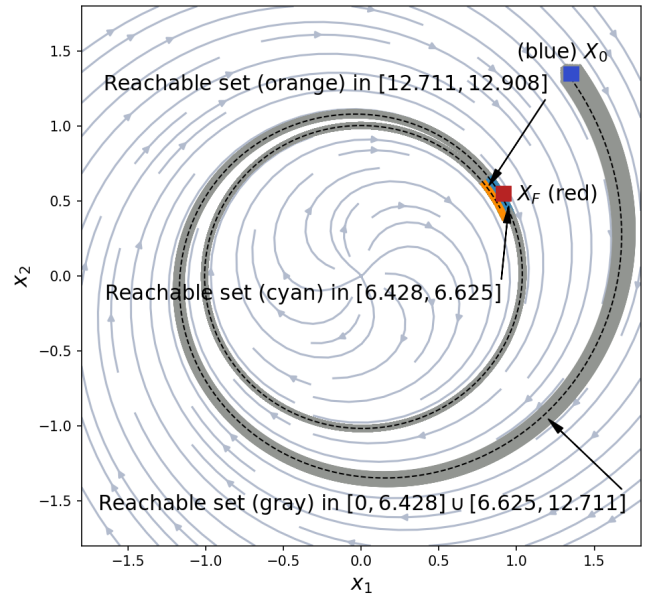


Fig. 5: Reachable set of the nonlinear system with stable limit cycle from initial set X_0 for duration $[0, 6.428] \cup [6.625, 12.711]$ (gray), estimated reach-time bound $I_0 = [6.428, 6.625]$ (cyan), $I_1 = [12.711, 12.908]$ (orange) with a simulated periodic reachable trajectory (black dashed lines).

respectively. By applying our method for the time reversed version of this system, we obtain the estimated backward reachable time intervals for X_F^1 and X_F^2 as $I_{\text{backward}}^1 = [0.655, 1.222]$ and $I_{\text{backward}}^2 = \emptyset$, which indicates that X_F^2 is unreachable from X_0 , and there are possible trajectories originating from X_0 that enter X_F^1 . This is indeed consistent with the simulation results as shown in Fig. 6.

C. Scalability

Example 6. (Cart-pole system [54]) Consider the dynamic of a cart-pole system as follows:

$$\dot{x} = \begin{bmatrix} \dot{p} \\ \dot{v} \\ \dot{\theta} \\ \dot{\omega} \end{bmatrix} = \begin{bmatrix} \frac{[F + m_p \sin(\theta)(l\omega^2 + g \cos(\theta))]}{m_c + m_p \sin(\theta)^2} \\ v \\ \omega \\ \frac{[-F \cos(\theta) - m_p l \omega^2 \cos(\theta) \sin(\theta) - (m_c + m_p)g \sin(\theta)]}{l(m_c + m_p \sin(\theta)^2)} \end{bmatrix}$$

where $m_c = 2, m_p = 1, l = 1$, and $g = 9.8065$.

We initialize the system with the state $X_0 = (0.8, 0.3, -\pi/4, 0.2)$ and the target set as $X_F = \{x \mid 10^{-4} \leq \|x\|_\infty \leq 10^{-2}, x \in X\}$, and apply our method to verify if a given LQR controller π_{LQR} can stabilize the system without collision. The system has principal eigenvalues $\lambda_{1,2} = -0.633 \pm 0.473j$ and $\lambda_{3,4} = -0.752 \pm 3.997j$ and a stable equilibrium at the origin. We first set the unsafe set as $X_U^1 = \{x \mid p + l \sin(\theta) > 1.3\}$, which represents a vertical wall. Our method outputs the reachable time bounds to the target set and the unsafe set as $I_F = [5.512, 10.413]$ and $I_U^1 = [0.157, 0.955]$ as visualized in the Fig. 7a.

When we change the unsafe set to $X_U^2 = \{x \mid p + l \sin(\theta) > 1.7\}$, the corresponding estimated reachable time interval is

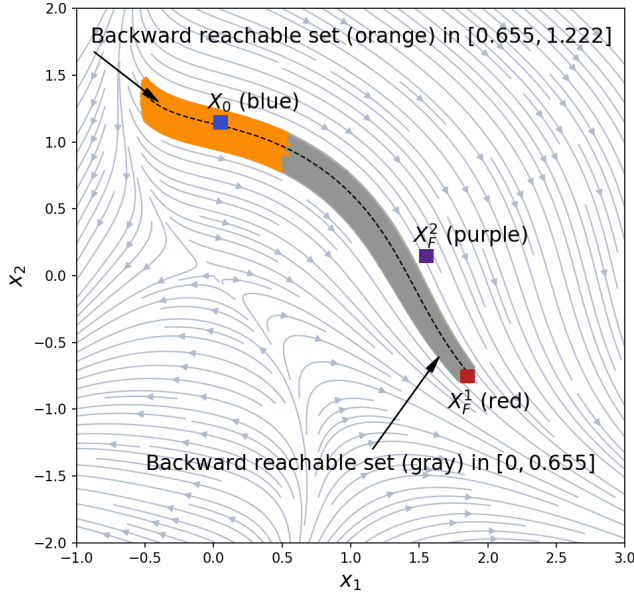


Fig. 6: Backward reachable set of the system with known eigenfunction from X_F^1 for duration $T = [0, 0.655]$ (gray), estimated backward reach-time bound $I_{backward} = [0.655, 1.222]$ (orange) with a simulated backward reachable trajectory (black dashed line).

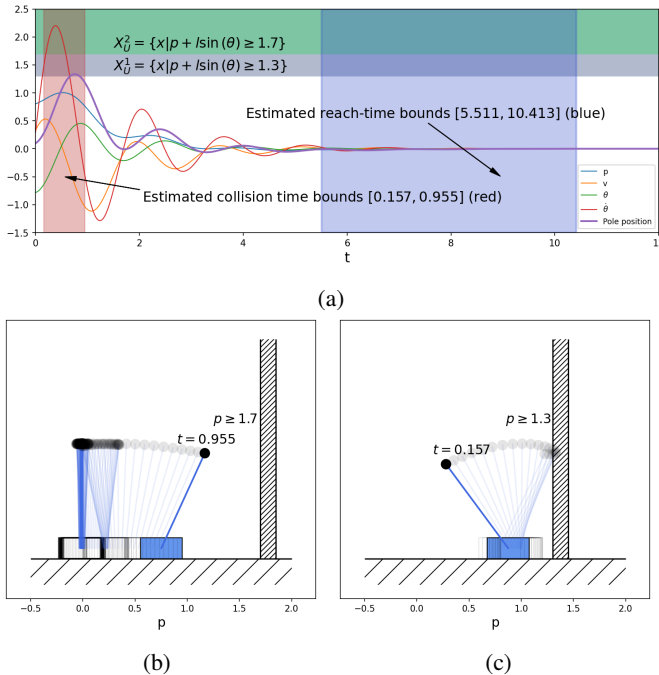


Fig. 7: Simulation of the Cart-pole system with LQR controller. (a) Convergence of the Cart-pole system under LQR control, with the estimated collision time bounds (red) and reach-time bounds (blue). (b) Motion snapshots within $T = [0.955, 10.413]$ demonstrate that the system finally stabilizes if there is no collision occurred. (c) Motion snapshots within the estimated collision time interval $I_U^1 = [0.157, 0.955]$.

$I_U^2 = \emptyset$. Following corollary 1, we can conclude that the unsafe set X_U^2 is unreachable from X_0 and the controller can safely drive the system to the equilibrium without collision with the wall. Fig. 7c depicts the simulation snapshots of the pole during the estimated unsafe time interval I_U^1 driven by the LQR controller. Indeed, the pole is shown to collide with the wall in this interval.

Example 7. (Multi-agent consensus system) Consider a multi-

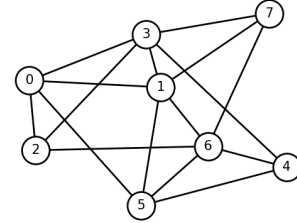


Fig. 8: A consensus system with 8 agents each with 2-dimensional states.

agent consensus problem corresponding to a graph \mathcal{G} , with vertex set $\mathcal{V} = \{0, \dots, n-1\}$ and edge set $\mathcal{E} = \{1, \dots, m\}$. The neighboring nodes of agent i is denoted by $N_i \subset \mathcal{V}$. The system state q is represented by the augmented state vector $q = [x_1, y_1, \dots, x_n, y_n]$. Each component of the state, such as x , follows the nonlinear distributed consensus protocol given by

$$\dot{x}_i = u_i = -\sigma_i(x_i) \sum_{j \in N_i} a_{ij}(x_i - x_j), \forall i \in \mathcal{V}$$

where $\sigma_i(\cdot)$ is continuous and positive for all $i \in \mathcal{V}$, and $a_{ij}(\cdot)$ is Lipschitz continuous for all $(i, j) \in \mathcal{E}$ with $a_{ij}(x) > 0$ when $x \neq 0$ and $a_{ij} = 0$. As a particular case illustrated in Fig. 8, we consider $n = 8$, $\sigma_i(z) = \frac{1}{1 + \exp(-z)}$ and $a_{ij}(\cdot) = r_{ij}[1.2 \tanh(\cdot) + \sin(\cdot)]$ with randomly sampled $r_{ij} \in (0, 1)$. By adding a linear term in x_i to the right-hand side of the system, we ensure that the origin is an asymptotically stable isolated equilibrium of this 16-dimensional system which in turn ensures convergence of numerical methods used for computation of Koopman eigenfunctions. As shown in [55], each agent's state will converge to some equilibrium point (x_i^*, y_i^*) if \mathcal{G} is connected and undirected and each $a_{ij}(\cdot)$ is an odd function. We are interested in this example to verify the convergence of each agent's state to its equilibrium, which is $(x_i^*, y_i^*) = (0, 0)$ in our settings, from arbitrary initial states.

As illustrated in Table III, we consider the cartesian product of 8 random chosen sets as the initial set $X_0 = \prod_{i=1}^8 X_0^i$. Furthermore, we define the target set as $X_F = \{q \mid 0.02 \leq \|q\|_\infty \leq 0.1, q \in X\}$ to verify each agent's state convergence around the equilibrium point $(0, 0)$, as well as unsafe sets $X_U^1 = \{q \mid \|q - 1.5\|_\infty \leq 0.5, q \in X\}$ and $X_U^2 = \{q \mid \|q + 1.25\|_\infty \leq 0.25, q \in X\}$. Under this configuration, our method estimates the reach time bound for X_F as $I = [5.855, 6.650]$, and the reach-time bounds estimation for two unsafe sets are both \emptyset , implying that all agent avoid entering the unsafe regions (due to corollary 1) while converging to the neighborhood X_F around the equilibrium point. The simulated

Agent	X_0^i		Principal Eigenvalues
	$x_i(0) \in$	$y_i(0) \in$	
1	[2.276, 2.476]	[-1.229, -1.029]	-0.442, -0.839
2	[-1.754, -1.554]	[1.784, 1.984]	-0.819, -0.509
3	[1.946, 2.146]	[-1.612, -1.412]	-0.719, -0.669
4	[-0.392, -0.192]	[0.996, 1.196]	-0.645, -0.565
5	[1.627, 1.827]	[-1.759, -1.559]	-0.442, -0.872
6	[0.725, 0.925]	[1.439, 1.639]	-0.779, -0.585
7	[0.149, 0.349]	[-1.776, -1.576]	-0.705, -0.672
8	[-2.422, -2.222]	[-1.192, -0.992]	-0.627 ± 0.004j

TABLE III: Initial sets and principal eigenfunctions of the multi-agent consensus system.

reachable sets of the system shown in Fig. 9 confirm the validity of our algorithm’s results.

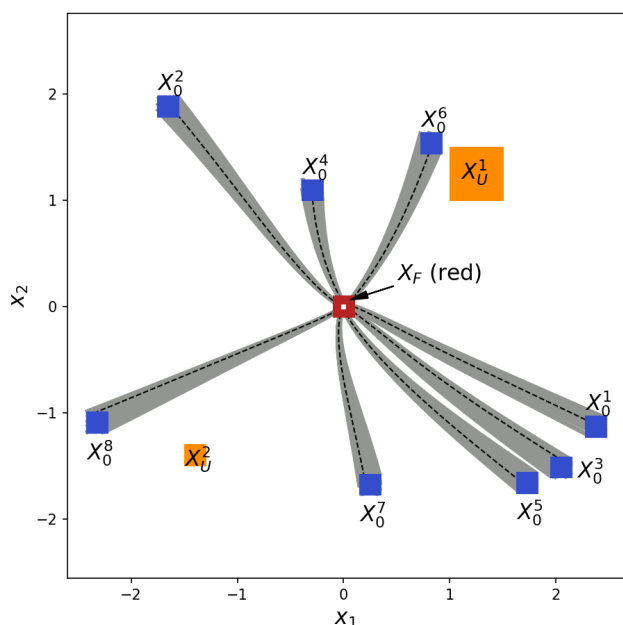


Fig. 9: Reachable sets (in gray) of agents from corresponding initial sets for duration $T = [0, 6.650]$ with simulated converging safe trajectories (black dashed lines).

VI. CONCLUSION AND DISCUSSION

This paper presents a methodology for verifying reachability based on the Koopman spectrum. The proposed method investigates the existence of feasible reachable time intervals to verify the reachability of systems, thereby avoiding the unnecessary computational overhead and conservatism arising from approximating the actual reachable sets. Numerical experiments showcase our method’s capability in verifying reachability between non-convex and even disconnected sets, over unbounded time horizons, and in the context of backward reachability. In addition, high-dimensional case studies illustrate the scalability of our method. Since our method is based on the over-approximation of the exact reachable time range, the non-emptiness of the intersection of time-to-reach bounds does not serve as a sufficient basis for

inferring reachability, although in such cases, the estimates can be combined with simulations to verify reachability. Our future research will focus on complementing the theory and seek its application when considering input control signals.

REFERENCES

- [1] S. Prajna and A. Rantzer, “Convex programs for temporal verification of nonlinear dynamical systems,” *SIAM Journal on Control and Optimization*, vol. 46, no. 3, pp. 999–1021, 2007.
- [2] R. Alur, T. Dang, and F. Ivančić, “Reachability analysis of hybrid systems via predicate abstraction,” in *Hybrid Systems: Computation and Control: 5th International Workshop, HSCC 2002 Stanford, CA, USA, March 25–27, 2002 Proceedings 5*. Springer, 2002, pp. 35–48.
- [3] E. Asarin, T. Dang, and A. Girard, “Reachability analysis of nonlinear systems using conservative approximation,” in *International Workshop on Hybrid Systems: Computation and Control*. Springer, 2003, pp. 20–35.
- [4] A. Tiwari, “Approximate reachability for linear systems,” in *International Workshop on Hybrid Systems: Computation and Control*. Springer, 2003, pp. 514–525.
- [5] E. Asarin, T. Dang, G. Frehse, A. Girard, C. Le Guernic, and O. Maler, “Recent progress in continuous and hybrid reachability analysis,” in *2006 IEEE Conference on Computer Aided Control System Design, 2006 IEEE International Conference on Control Applications, 2006 IEEE International Symposium on Intelligent Control*. IEEE, 2006, pp. 1582–1587.
- [6] S. Bansal, M. Chen, S. Herbert, and C. J. Tomlin, “Hamilton-jacobi reachability: A brief overview and recent advances,” in *2017 IEEE 56th Annual Conference on Decision and Control (CDC)*. IEEE, 2017, pp. 2242–2253.
- [7] J. Lygeros, “On reachability and minimum cost optimal control,” *Automatica*, vol. 40, no. 6, pp. 917–927, 2004.
- [8] I. M. Mitchell *et al.*, “A toolbox of level set methods,” *UBC Department of Computer Science Technical Report TR-2007-11*, vol. 1, p. 6, 2007.
- [9] R. E. Allen, A. A. Clark, J. A. Starek, and M. Pavone, “A machine learning approach for real-time reachability analysis,” in *2014 IEEE/RSJ International conference on intelligent robots and systems*. IEEE, 2014, pp. 2202–2208.
- [10] S. Bansal and C. J. Tomlin, “Deepreach: A Deep Learning approach to high-dimensional reachability,” in *2021 IEEE International Conference on Robotics and Automation (ICRA)*. IEEE, 2021, pp. 1817–1824.
- [11] S. Sankaranarayanan, H. B. Sipma, and Z. Manna, “Constructing invariants for hybrid systems,” in *Hybrid Systems: Computation and Control: 7th International Workshop, HSCC 2004, Philadelphia, PA, USA, March 25–27, 2004. Proceedings 7*. Springer, 2004, pp. 539–554.
- [12] K. Ghorbal, A. Sogokon, and A. Platzer, “A hierarchy of proof rules for checking positive invariance of algebraic and semi-algebraic sets,” *Computer Languages, Systems & Structures*, vol. 47, pp. 19–43, 2017.
- [13] A. Tiwari and G. Khanna, “Nonlinear systems: Approximating reach sets,” in *International Workshop on Hybrid Systems: Computation and Control*. Springer, 2004, pp. 600–614.
- [14] S. Prajna, A. Jadbabaie, and G. J. Pappas, “A framework for worst-case and stochastic safety verification using barrier certificates,” *IEEE Transactions on Automatic Control*, vol. 52, no. 8, pp. 1415–1428, 2007.
- [15] S. Prajna and A. Jadbabaie, “Safety verification using barrier certificates,” *HSCC*.
- [16] A. Ghaffari, I. Abel, D. Ricketts, S. Lerner, and M. Krstić, “Safety verification using barrier certificates with application to double integrator with input saturation and zero-order hold,” in *2018 Annual American Control Conference (ACC)*. IEEE, 2018, pp. 4664–4669.
- [17] M. Althoff, G. Frehse, and A. Girard, “Set propagation techniques for reachability analysis,” *Annual Review of Control, Robotics, and Autonomous Systems*, vol. 4, pp. 369–395, 2021.
- [18] M. Althoff and N. Kochdumper, “Cora 2016 manual,” *TU Munich*, vol. 85748, 2016.
- [19] S. Bogomolov, M. Forets, G. Frehse, K. Potomkin, and C. Schilling, “Juliareach: a toolbox for set-based reachability,” in *Proceedings of the 22nd ACM International Conference on Hybrid Systems: Computation and Control*, 2019, pp. 39–44.

- [20] X. Chen, E. Ábrahám, and S. Sankaranarayanan, “Flow*: An analyzer for non-linear hybrid systems,” in *Computer Aided Verification: 25th International Conference, CAV 2013, Saint Petersburg, Russia, July 13-19, 2013. Proceedings* 25. Springer, 2013, pp. 258–263.
- [21] H. Abbas, G. Fainekos, S. Sankaranarayanan, F. Ivančić, and A. Gupta, “Probabilistic temporal logic falsification of cyber-physical systems,” *ACM Transactions on Embedded Computing Systems (TECS)*, vol. 12, no. 2s, pp. 1–30, 2013.
- [22] S. Kong, S. Gao, W. Chen, and E. Clarke, “dreach: δ -reachability analysis for hybrid systems,” in *Tools and Algorithms for the Construction and Analysis of Systems: 21st International Conference, TACAS 2015, Held as Part of the European Joint Conferences on Theory and Practice of Software, ETAPS 2015, London, UK, April 11-18, 2015, Proceedings 21*. Springer, 2015, pp. 200–205.
- [23] A. Abate, D. Ahmed, A. Edwards, M. Giacobbe, and A. Peruffo, “Fossil: a software tool for the formal synthesis of lyapunov functions and barrier certificates using neural networks,” in *Proceedings of the 24th international conference on hybrid systems: computation and control*, 2021, pp. 1–11.
- [24] X. Chen and S. Sankaranarayanan, “Reachability analysis for cyber-physical systems: Are we there yet?” in *NASA Formal Methods Symposium*. Springer, 2022, pp. 109–130.
- [25] S. Coogan, “Mixed monotonicity for reachability and safety in dynamical systems,” in *2020 59th IEEE Conference on Decision and Control (CDC)*. IEEE, 2020, pp. 5074–5085.
- [26] J. Maidens and M. Arcak, “Exploiting symmetry for discrete-time reachability computations,” *IEEE Control Systems Letters*, vol. 2, no. 2, pp. 213–217, 2018.
- [27] H. Sibai, N. Mokhlesi, C. Fan, and S. Mitra, “Multi-agent safety verification using symmetry transformations,” in *International Conference on Tools and Algorithms for the Construction and Analysis of Systems*. Springer, 2020, pp. 173–190.
- [28] X. Chen and S. Sankaranarayanan, “Decomposed reachability analysis for nonlinear systems,” in *2016 IEEE Real-Time Systems Symposium (RTSS)*. IEEE, 2016, pp. 13–24.
- [29] C. Daws and S. Tripakis, “Model checking of real-time reachability properties using abstractions,” in *International Conference on Tools and Algorithms for the Construction and Analysis of Systems*. Springer, 1998, pp. 313–329.
- [30] D. Cattaruzza, A. Abate, P. Schrammel, and D. Kroening, “Unbounded-time analysis of guarded lti systems with inputs by abstract acceleration,” in *Static Analysis: 22nd International Symposium, SAS 2015, Saint-Malo, France, September 9-11, 2015, Proceedings 22*. Springer, 2015, pp. 312–331.
- [31] A. Devonport and M. Arcak, “Data-driven reachable set computation using adaptive gaussian process classification and monte carlo methods,” in *2020 American control conference (ACC)*. IEEE, 2020, pp. 2629–2634.
- [32] A. Devonport, F. Yang, L. El Ghaoui, and M. Arcak, “Data-driven reachability analysis with christoffel functions,” in *2021 60th IEEE Conference on Decision and Control (CDC)*. IEEE, 2021, pp. 5067–5072.
- [33] A. Alanwar, A. Koch, F. Allgöwer, and K. H. Johansson, “Data-driven reachability analysis using matrix zonotopes,” in *Learning for Dynamics and Control*. PMLR, 2021, pp. 163–175.
- [34] —, “Data-driven reachability analysis from noisy data,” *IEEE Transactions on Automatic Control*, 2023.
- [35] J. C. Willems, P. Rapisarda, I. Markovsky, and B. L. De Moor, “A note on persistency of excitation,” *Systems & Control Letters*, vol. 54, no. 4, pp. 325–329, 2005.
- [36] B. O. Koopman, “Hamiltonian systems and transformation in hilbert space,” *Proceedings of the National Academy of Sciences*, vol. 17, no. 5, pp. 315–318, 1931.
- [37] P. J. Schmid, “Dynamic mode decomposition and its variants,” *Annual Review of Fluid Mechanics*, vol. 54, no. 1, pp. 225–254, 2022.
- [38] I. Mezić, “On numerical approximations of the koopman operator,” *Mathematics*, vol. 10, no. 7, p. 1180, 2022.
- [39] S. A. Deka, S. S. Narayanan, and U. Vaidya, “Path-integral formula for computing koopman eigenfunctions,” in *2023 62nd IEEE Conference on Decision and Control (CDC)*. IEEE, 2023, pp. 6641–6646.
- [40] A. Mauroy, I. Mezić, and J. Moehlis, “Isostables, isochrons, and koopman spectrum for the action-angle representation of stable fixed point dynamics,” *Physica D: Nonlinear Phenomena*, vol. 261, pp. 19–30, 2013.
- [41] S. A. Deka and D. V. Dimarogonas, “Supervised learning of lyapunov functions using laplace averages of approximate koopman eigenfunctions,” *IEEE Control Systems Letters*, 2023.
- [42] S. A. Deka, A. M. Valle, and C. J. Tomlin, “Koopman-based Neural Lyapunov functions for general attractors,” in *IEEE 61st Conference on Decision and Control (CDC)*. IEEE, 2022, pp. 5123–5128.
- [43] S. Bak, S. Bogomolov, P. S. Duggirala, A. R. Gerlach, and K. Potomkin, “Reachability of black-box nonlinear systems after koopman operator linearization,” *IFAC-PapersOnLine*, vol. 54, no. 5, pp. 253–258, 2021.
- [44] S. Bak, S. Bogomolov, B. Hency, N. Kochdumper, E. Lew, and K. Potomkin, “Reachability of koopman linearized systems using random fourier feature observables and polynomial zonotope refinement,” in *International Conference on Computer Aided Verification*. Springer, 2022, pp. 490–510.
- [45] D. Goswami and D. A. Paley, “Bilinearization, reachability, and optimal control of control-affine nonlinear systems: A koopman spectral approach,” *IEEE Transactions on Automatic Control*, vol. 67, no. 6, pp. 2715–2728, 2021.
- [46] B. Umathe, D. Tellez-Castro, and U. Vaidya, “Reachability analysis using spectrum of koopman operator,” *IEEE Control Systems Letters*, vol. 7, pp. 595–600, 2022.
- [47] I. Mezić, “Spectrum of the koopman operator, spectral expansions in functional spaces, and state-space geometry,” *Journal of Nonlinear Science*, pp. 1–55, 2019.
- [48] Y. Lan and I. Mezić, “Linearization in the large of nonlinear systems and koopman operator spectrum,” *Physica D: Nonlinear Phenomena*, vol. 242, no. 1, pp. 42–53, 2013.
- [49] V. I. Arnold, *Geometrical methods in the theory of ordinary differential equations*. Springer Science & Business Media, 2012, vol. 250.
- [50] R. Mohr and I. Mezić, “Koopman principle eigenfunctions and linearization of diffeomorphisms,” *arXiv preprint arXiv:1611.01209*, 2016.
- [51] M. D. Kvalheim and S. Revzen, “Existence and uniqueness of global koopman eigenfunctions for stable fixed points and periodic orbits,” *Physica D: Nonlinear Phenomena*, vol. 425, p. 132959, 2021.
- [52] E. M. Bollt, “Geometric considerations of a good dictionary for koopman analysis of dynamical systems: Cardinality, primary eigenfunction, and efficient representation,” *Communications in Nonlinear Science and Numerical Simulation*, vol. 100, p. 105833, 2021.
- [53] A. C. W. Cooper *et al.*, “Programming with linear fractional functionals,” *Naval Research logistics quarterly*, vol. 9, no. 3, pp. 181–186, 1962.
- [54] R. Tedrake, “Underactuated robotics: Learning, planning, and control for efficient and agile machines course notes for mit 6.832,” *Working draft edition*, vol. 3, no. 4, p. 2, 2009.
- [55] M. Andreasson, D. V. Dimarogonas, H. Sandberg, and K. H. Johansson, “Distributed control of networked dynamical systems: Static feedback, integral action and consensus,” *IEEE Transactions on Automatic Control*, vol. 59, no. 7, pp. 1750–1764, 2014.